

OraPO: Oracle-educated Reinforcement Learning for Data-efficient and Factual Radiology Report Generation

Zhuoxiao Chen^{1,2†}, Hongyang Yu^{1*}, Ying Xu¹, Yadan Luo², Long Duong¹, Yuan-Fang Li^{1*}
¹Oracle Health & AI, ²The University of Queensland

{ivan.chen, hongyang.yu, ying.x.xu, long.duong, yuanfang.li}@oracle.com

{zhuoxiao.chen, y.luo}@uq.edu.au

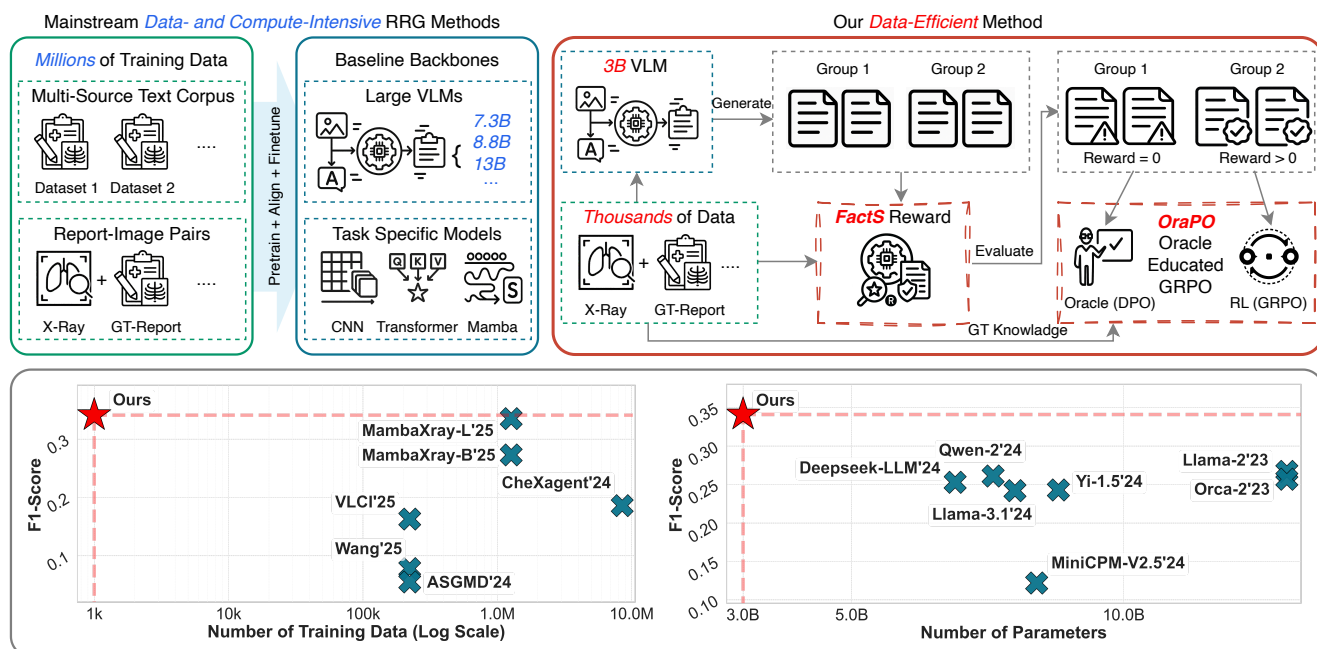


Figure 1. Illustration of mainstream data/compute-intensive pipelines (upper-left) versus our data-efficient pipeline (upper-right). Bottom: our method achieves the **SOTA performance for RRG** with **less than 0.1%** of the training samples (vs. 1.27 M) used by best-performing baselines and a **much smaller model**, demonstrating strong performance under tight data and compute budgets.

Abstract

Radiology report generation (RRG) aims to automatically produce clinically faithful reports from chest X-ray images. Prevailing work typically follows a **scale-driven paradigm**, by multi-stage training over large paired corpora and oversized backbones, making pipelines highly data- and compute-intensive. In this paper, we propose Oracle-educated GRPO (**OraPO**) with a FactScore-based reward (**FactS**) to tackle the RRG task under constrained budgets. OraPO enables single-stage, RL-only training by

converting failed GRPO explorations on rare or difficult studies into direct preference supervision via a lightweight oracle step. FactS grounds learning in diagnostic evidence by extracting atomic clinical facts and checking entailment against ground-truth labels, yielding dense, interpretable sentence-level rewards. Together, OraPO and FactS create a compact and powerful framework that significantly improves learning efficiency on clinically challenging cases, setting the **new SOTA performance** on the CheXpert Plus dataset (0.341 in F1) with **2–3 orders of magnitude less training data** using a **small base VLM** on modest hardware.

[†] Work done during an internship at Oracle Health & AI. ^{*} Joint senior authors.

1. Introduction

Radiology report generation (RRG) from chest X-rays aims to turn imaging evidence into a clinically usable narrative. This is a complex multimodal task that couples disease prediction with free-text report generation, linking detected visual findings (e.g. edema, pleural effusion, and pneumothorax) to clear sentences that describe their presence, details, location, and severity. Automating this task matters in practice: the large imaging volumes and backlogs place serious strains on healthcare services and delay patient care, while radiologist staffing remains insufficient. For example, England reports a 29% radiology consultant shortfall alongside sustained vacancies [48], while in the United States there are about 14,000 openings but only 1,150 resident graduates annually [53]. In this context, AI-assisted drafting has begun to show measurable efficiency gains. A recent study [1] reported that using draft reports generated by large language models (LLMs) reduced reporting time by 24%. Given its practical importance, automated radiology report generation has rapidly become an active research area aimed at easing radiologists’ workload and streamlining workflows in hospitals and clinics.

Mainstream RRG methods typically rely on supervised fine-tuning (SFT) via multi-stage training on large corpora and/or scaling up backbone size (Fig. 1, upper-left). The multi-stage training paradigm usually follows three phases: domain-specific pre-training, image–text alignment, and task-specific fine-tuning, where the first two are usually trained on combinations of large-scale, multi-source datasets such as medical textbooks, real radiology reports including but not limited to MIMIC-CXR [29], IU X-ray [17] and CheXpert Plus [8], often for dozens of epochs [62, 64]. Notably, both CheXpert Plus and MIMIC-CXR include training splits **exceeding 200K** image-report pairs. In addition, there is a recent trend of adopting large vision-language models (VLMs) with >13B parameters for SFT, demanding meticulous data curation and substantial GPU budgets [30, 32].

Recently, *Group Relative Policy Optimisation* (GRPO) has emerged as a strong and compute-efficient RL-based learning algorithm for many hard problems with verifiable rewards. Its efficiency comes from two fronts: (i) lower memory/compute by dispensing with the trainable value critic and instead computing group-normalised advantages from the relative rewards of multiple samples [31, 45]; and (ii) a simplified training recipe that enables “RL-only” regimes (i.e., without costly SFT/alignment), avoiding massive pre-training/alignment corpora [10, 16, 54].

However, applying GRPO to the RRG task reveals two challenges. Challenge (i): we observe that vanilla GRPO often produces all-zero reward groups early in training (e.g. 30% in the first 50 steps as shown in Fig. 2 left), causing vanishing gradients and wasted rollouts. Recent variants at-

tempt to fix this by resampling until a non-zero reward appears [75] or by enlarging the group size [55], both of which are still suboptimal due to *increased cost* of more rollouts. Another line interleaves SFT with RL to maintain gradient flow, yet still leaves low-quality rollouts unused, wasting costly sampling [11, 37, 39, 40, 76]. Challenge (ii): vanilla GRPO requires readily verifiable scalar rewards. Unlike multiple-choice QA, maths, or coding, where the reward is typically a binary final-answer check, radiology reports are long-form, multi-fact, and must be consistent across sentences, making reward design both critical and difficult. In practice, RLHF-style RRG work often uses reference-overlap metrics that mainly capture *fluency/surface similarity* (e.g. BLEU/CIDEr [33, 47]) or a *report-level clinical metric* [44, 74, 80]. These proxies under-penalise sentence-level factual errors and cross-sentence contradictions, yielding fluent yet clinically misleading narratives (missed positives, unsupported claims). Hence, a reward must be able to assess factual correctness of each statement of a radiology report in an efficient manner.

In this paper, we propose *Oracle-educated Group Relative Policy Optimisation*: **OraPO**, a novel RL-based learning algorithm that tackles RRG’s challenges in a data- and compute-efficient manner. OraPO addresses Challenge (i) of GRPO by dynamically injecting oracle supervision (i.e. ground-truth) for groups with *all-zero* rewards and teaching the policy to avoid repeating low-quality generations. Specifically, When a sampled group yields *all-zero* rewards (group 1 in Fig. 1, upper-right), OraPO triggers a lightweight Direct Preference Optimisation (DPO) update that directly prefers the ground-truth report over the zero-reward rollouts as *ready-made negatives*, without extra compute or annotations. This converts failed exploration on difficult cases (hard or low-prevalence studies) into useful gradients, moving the policy away from low-quality modes and toward the ground-truth. We also introduce a simple adaptive mixing weight to increase DPO’s influence when zero-reward groups are frequent, which gradually tapers once GRPO provides informative advantages, making OraPO salvage otherwise wasted batches, stabilise training, and accelerate convergence.

Moreover, to provide OraPO with clinically faithful supervision, we introduce a **FactScore**-based reward [42] designed to address Challenge (ii). We treat the generated report as its own rationale, extract *atomic clinical facts*, and test their *entailment* against the ground-truth label set. Facts that support a label contribute positively; unsupported or contradictory labels incur penalties, yielding a dense, interpretable per-label reward. This stands in sharp contrast to the original GRPO reward, which assigns reward solely to the final answer while treating the reasoning trace largely as a byproduct of generation, without ensuring it is factually grounded or consistently aligned with the answer. Our

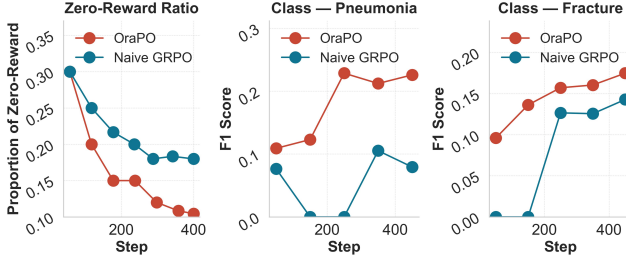


Figure 2. *Left*: Cumulative proportion of *zero-reward* batches (reward batch mean = 0) vs. training step on CheXpert Plus [62]. **OraPO** suppresses zero-reward frequency faster than naïve GRPO. *Centre/Right*: Class-level F1 on the CheXpert Plus validation set [62] across checkpoints for two *clinically challenging and rare* classes: **Pneumonia** (2.70%) and **Fracture** (4.05%). **OraPO** learns earlier and maintains higher F1 than naïve GRPO.

reward design ensures the generated report (serving in lieu of reasoning trace) not only produces correct cognitive reasoning trace similar to that of an experienced radiologist but also yields correct diagnostic findings, which is crucial in domains such as healthcare in which safety is of paramount importance.

In summary, our contributions are **threefold**:

1. We present **OraPO**, an Oracle (DPO) educated GRPO that turns failed explorations into direct preference supervision and uses an adaptive mixing schedule to emphasize DPO when GRPO’s signal vanishes, significantly improving data- and compute-efficiency. To the best of our knowledge, this is the **first** work that integrates direct preference learning with GRPO-based RL for efficient training.
2. We design a **Facts Reward** for RL, performing fact-level entailment against ground-truth labels, yielding dense, interpretable feedback that aligns reports with diagnostic facts while avoiding long reasoning traces.
3. OraPO sets the new SOTA performance for RRG, surpassing the previous best model in terms of clinical effectiveness F1 score. This is achieved while being exceptionally data-efficient, with **2–3 orders of magnitude less training data**. OraPO is trained on only **1K** samples. In contrast, the current best model MambaXray-L is trained on **1.27M** samples and all the other models are trained on at least 223K samples. At the same time, OraPO is also compute-efficient: it is based on QWen2.5-VL-3B, a moderately-sized VLM on modest hardware (**4x A10 GPUs**).

2. Related Work

Automatic Radiology Report Generation (RRG) aims to turn imaging studies (*e.g.*, chest X-rays) into clinically usable free-text reports. Early approaches adopted seq2seq networks (*e.g.*, CNN-RNN and Transformer) [13, 28] for

training on large paired corpora such as MIMIC-CXR [29]. Recent work advances three fronts: (i) *knowledge- and rule-guided generation*, which injects medical priors to curb hallucination [6] and performs disease-aware image–text alignment for trustworthy text [50]; (ii) *leveraging prior studies and multi-view images* to improve coverage and consistency [22, 36]; and (iii) *scaling/standardizing with pre-training*, releasing multi-stage pre-training recipes [22, 62]. In parallel, LLM-driven RRG explores instruction-tuned or preference-aligned training [32, 35]. Despite progress, these approaches often rely on large paired corpora and/or costly computation resources, leading to deficiency.

Group Relative Policy Optimisation (GRPO) is a critic-free, reinforcement learning *objective* for generative LLMs, introduced in *DeepSeekMath* [54]. It samples multiple completions per prompt, computes group-normalised advantages from relative rewards, and updates the policy with clipped ratios to a frozen reference; removing the critic reduces memory/compute versus PPO while preserving stability [21, 31, 45, 54]. Recent variants mainly target optimisation stability: DR.GRPO [38] mitigates length bias and skewed group rewards; CISPO [9] clips importance-sampling weights; GSPO [77] adopts sequence-level clipping for MoE; DAPO [75] resamples until a non-zero reward appears. However, these methods were not designed to improve data efficiency: most target optimisation stability while leaving data volume and training epochs essentially unchanged, and some of them often increase sampling/compute [55, 59, 75].

Direct Preference Optimisation (DPO) trains a policy from *preference pairs* to prefer the chosen response over the rejected one [79]. Recent variants streamline or robustify this recipe: SimPO [41] applies length-normalised mean log-probabilities with a simplified reference; Cal-DPO [67] calibrates the implicit reward to human scales; ORPO [24] drops the reference via an odds-ratio objective integrated into SFT; and KTO [29] learns from unary thumbs-up/down signals instead of pairs. In our RRG framework, DPO naturally serves as an *oracle step* inside **OraPO** to convert those failed GRPO rollouts into useful preference updates against the ground-truth, leading to data- and compute-efficient learning.

3. Methodology

In this section, we first introduce the background of Group Relative Policy Optimisation (GRPO) and Direct Preference Optimisation (DPO) (§3.1). We then identify a failure mode of GRPO in radiology report generation (RRG), when a pretrained model produces many low-quality groups (*e.g.*, zero rewards) that yield little or no gradient. This observation motivates our proposed **OraPO** algorithm, which efficiently converts such failed explorations into preference supervision (§3.2). Finally, we design the **Facts Reward**,

a fact-level entailment signal that aligns reports with diagnostic labels and provides dense, interpretable feedback for reinforcement learning (§3.3).

3.1. Preliminaries

Group Relative Policy Optimisation (GRPO). GRPO [21, 54] is a computation- and memory-efficient RL objective for aligning generative models (LLMs/VLMs), introduced for reasoning-heavy settings and now used broadly because of its efficient critic-free design and proven effectiveness. It replaces the value critic with *group-normalized* advantages computed among multiple completions sampled for the same input. Given a study–prompt pair (x, p) , the policy π_θ draws a group of K sequences $\{\hat{y}_j\}_{j=1}^K \sim \pi_\theta(\cdot | x, p)$ and receives scalar rewards $r_j = r(x, \hat{y}_j)$. GRPO forms a group baseline and scale,

$$\bar{r} = \frac{1}{K} \sum_{j=1}^K r_j, \quad \sigma = \sqrt{\frac{1}{K} \sum_{j=1}^K (r_j - \bar{r})^2 + \varepsilon}, \quad (1)$$

and defines the group-normalised advantage:

$$A_j = \frac{r_j - \bar{r}}{\sigma}. \quad (2)$$

Let the proximal policy optimisation (PPO) ratio be:

$$\rho_j = \exp(\log \pi_\theta(\hat{y}_j | x, p) - \log \pi_{\theta_{\text{old}}}(\hat{y}_j | x, p)), \quad (3)$$

where θ_{old} denotes the parameters of the behaviour policy used to sample the current group (*i.e.*, the parameters before the update). Then the GRPO loss over a batch is defined as:

$$\begin{aligned} \mathcal{L}_{\text{GRPO}} = & -\mathbb{E} \left[\min(\rho_j A_j, \text{clip}(\rho_j, 1 - \epsilon, 1 + \epsilon) A_j) \right] \\ & + \lambda_{\text{KL}} \mathbb{E} [\text{KL}(\pi_\theta(\cdot | x, p) \| \pi_{\text{ref}}(\cdot | x, p))], \end{aligned} \quad (4)$$

where ϵ is the clipping threshold, $\lambda_{\text{KL}} \geq 0$ controls regularization toward a frozen reference policy π_{ref} . In practice, GRPO samples K completions per prompt, computes r_j , normalizes within-group to obtain A_j , and updates π_θ with the clipped-ratio objective in (4), thereby achieving critic-free policy optimisation.

Direct Preference Optimisation (DPO). DPO [79] is a widely used, preference-alignment objective for generative LLMs/VLMs. It updates the policy to prefer *chosen* completions over *rejected* ones relative to a frozen reference model. Given a preference dataset $\mathcal{P} = \{(x, p, y^+, y^-)\}$, where y^+ is preferred to y^- for the same input–prompt pair (x, p) , DPO maximizes the log-probability margin of the preferred sample after subtracting the reference log-probabilities. Let π_θ be the trainable policy and π_{ref} the frozen reference. The expectation below is taken over preference pairs drawn from \mathcal{P} . With temperature $\tau > 0$, define

$$\Delta^+ = \log \pi_\theta(y^+ | x, p) - \log \pi_{\text{ref}}(y^+ | x, p), \quad (5)$$

$$\Delta^- = \log \pi_\theta(y^- | x, p) - \log \pi_{\text{ref}}(y^- | x, p), \quad (6)$$

and the DPO loss

$$\mathcal{L}_{\text{DPO}} = -\mathbb{E} \left[\log \sigma(\tau (\Delta^+ - \Delta^-)) \right], \quad (7)$$

where $\sigma(\cdot)$ is the logistic sigmoid.

3.2. OraPO: Oracle-educated GRPO

Exploration Failure of GRPO in RRG. On radiology report generation, applying vanilla GRPO to a base VLM with limited radiology knowledge often fails to explore productively. The root reason is that the base model carries very limited domain knowledge about radiology. Most base VLMs are pre-trained on general vision–language corpora and tasks, for example, everyday-image captioning on MS COCO [34] and open-domain visual question answering on VQA v2 [19], rather than medical imaging and reporting. Hence, it tends to miss or misstate rare and/or clinically challenging findings (*e.g.*, small pneumothorax, subtle interstitial edema, or linear atelectasis) when asked to produce clinical narratives. For many chest X-ray inputs, the sampled group of completions is uniformly low quality with near-zero rewards. Thus, the policy receives little learning signal to drive effective exploration.

Empirically, before any domain-specific fine-tuning, the pretrained backbone attains only 0.034 macro-F1 (Tab. 3) on clinical effectiveness. As shown in Fig. 2 (left), in the first 50 optimisation steps approximately 30% of groups have all rewards equal to zero. Under the GRPO construction, such groups give $\bar{r} \approx 0$ and $\sigma \approx \varepsilon$, so $A_j = \frac{r_j - \bar{r}}{\sigma} \approx 0$ for all j . Consequently, the clipped-ratio term in Eq. (4) contributes essentially no gradient, and the update is dominated by the KL regularizer to π_{ref} rather than by task reward. In effect, the optimizer wastes GPU resources by sampling K completions per prompt without extracting useful signals, which both slows convergence and squanders valuable compute.

Zero-Reward Rate (ZRR). To resolve GRPO’s exploration failure on RRG, we first *detect* when a prompt yields little or no usable signal, then adapt learning accordingly. We introduce a *Zero-Reward Rate (ZRR)* that quantifies, per prompt, how severely GRPO has stalled.

For prompt x_i with a GRPO group of K completions $\{\hat{y}_{i,j}\}_{j=1}^K$ and rewards $r_{i,j} \in [0, 1]$, define the raw zero-reward rate:

$$z_i = \frac{1}{K} \sum_{j=1}^K \mathbf{1}[r_{i,j} = 0], \quad (8)$$

here, $z_i = 1$ indicates an all-zero group (no learning signal) and $z_i = 0$ indicates at least one non-zero reward (GRPO has exploitable signal). To reduce step-to-step noise, we maintain an exponential moving average (EMA):

$$\tilde{z}_i^{(t)} = \alpha \tilde{z}_i^{(t-1)} + (1 - \alpha) z_i^{(t)}, \quad \alpha \in [0, 1), \quad (9)$$

computed per prompt (or per minibatch) at step t .

We then map $\tilde{z}_i^{(t)}$ to a bounded, monotonic mixing weight that will later control how much oracle education to apply:

$$w_i^{(t)} = \text{clip}\left(w_{\min} + (w_{\max} - w_{\min})[\tilde{z}_i^{(t)}]^\gamma, w_{\min}, w_{\max}\right), \quad (10)$$

where $w_{\min} \leq w_i^{(t)} \leq w_{\max}$ enforces a narrow operating range for stability. The exponent γ shapes sensitivity: larger γ concentrates education on the most severe failures while leaving ordinary prompts to GRPO.

Integrating Two Objectives. With the ZRR-derived weight $w_i^{(t)}$ in hand, we modulate learning per prompt: when GRPO provides usable signal ($w_i^{(t)}$ is small), we emphasise exploration and exploitation; when GRPO stalls ($w_i^{(t)}$ is large), we shift toward direct education via preference alignment. We combine both signals in a single objective over a batch of size B :

$$\mathcal{L}_{\text{OraPO}} = \frac{1}{B} \sum_{i=1}^B \left[(1 - w_i^{(t)}) \mathcal{L}_{\text{GRPO}}(x_i, p_i) + w_i^{(t)} \mathcal{L}_{\text{DPO}}(x_i, p_i) \right], \quad (11)$$

where $\mathcal{L}_{\text{GRPO}}(x_i, p_i)$ is the GRPO loss in Eq. (4) evaluated on the sampled completions (x_i, p_i) , and $\mathcal{L}_{\text{DPO}}(x_i, p_i)$ is the DPO loss in Eq. (7) computed on preference pairs associated with the same prompt (x_i, p_i) . We set the positive to the ground-truth report y_i^* and take negatives from all other model completions:

$$y_i^+ = y_i^*, \quad y_i^- \in \{\hat{y}_{i,j}\}_{j=1}^K \sim \pi_\theta(\cdot | x_i, p_i) \quad (12)$$

where $\{\hat{y}_{i,j}\}_{j=1}^K$ is the entire group sampled from $\pi_\theta(\cdot | x_i, p_i)$. We then instantiate $\mathcal{L}_{\text{DPO}}(x_i, p_i)$ by applying Eq. (7) over pairs $\{(x_i, p_i, y_i^+, y_i^-)\}$. This construction reuses low-reward GRPO generation as a preference negative rather than discarding them. As a result, it enables DPO training without requiring any additional hard-negative mining or auxiliary generators. Generated rollouts with zero or low rewards serve as high-quality, domain-specific negative samples that are otherwise difficult to obtain manually.

Intuitively, a **high ZRR** flags failure cases where preference *education* must lead. OraPO responds by increasing $w_i^{(t)}$ and applying DPO updates that teach the policy to reject the sampled negatives and align with the ground-truth report. This converts groups into labeled preferences and supplies gradients exactly when GRPO has none/few. A **low ZRR** indicates that GRPO is uncovering usable reward. This can happen on simpler studies, and it also emerges after DPO has taught the model the cues for difficult findings (e.g., small apical pneumothorax or subtle interstitial

edema), enabling a shift from education to exploration and exploitation. In practice, we observe the intended training dynamic, as shown in Fig. 2: early training is education-heavy with larger ratio of zero-reward groups $\rightarrow w^{(t)}$, then $w^{(t)}$ gradually declines as the policy learns and GRPO takes over.

What does OraPO Buy Us? As shown in Fig. 2, **OraPO** drives down the zero-reward ratio faster, and to a lower plateau than naïve GRPO, implying fewer wasted rollouts and more gradient-carrying updates. Corroborating this, the class-level performance curves for *Pneumonia* and *Fracture* (clinically challenging, low-prevalence labels) show that **OraPO** improves *earlier* and sustains *higher* F1 across checkpoints. The coupled trend (rapid ZRR decline \rightarrow earlier F1 lift on hard classes) indicates that DPO is converting failed exploration into effective supervision rather than merely stabilising optimisation, yielding both better sample efficiency and stronger performance where it matters.

This initiates a **self-reinforcing data flywheel**: as the model learns through Oracle education and GRPO’s exploration–exploitation process, it produces increasingly informative negative samples. These, in turn, carry higher reward signals, pushing the model to achieve even greater rewards and completing a positive, compounding feedback cycle.

3.3. FactScore-based Reward Design

OraPO needs a reward that is reliable and efficient to compute. Many RL-based RRG approaches optimize report-level proxies or embedding similarity, which favors fluent paraphrases over verifiable clinical facts and can yield plausible but clinically incorrect narratives. We introduce a FactScore-based reward (**FACTS**) that treats the report as its own rationale: extract atomic clinical facts and test each against the ground-truth label set to produce a dense, fact-entailment signal for reinforcement learning.

Step 1: Extract atomic clinical facts. Inspired by FactScore [42], we define a *fact* as an atomic, verifiable clinical statement (e.g. finding, attribute, and optionally location), for instance, “no pleural effusion”, “linear atelectasis at the left base”. Given a generated report \hat{y}_i , we prompt GPT-4.1 [49] to extract a set of atomic facts:

$$\mathcal{F}(\hat{y}_i) = \{s_{i,k}\}_{k=1}^{K_i}, \quad (13)$$

ensuring each $s_{i,k}$ is concise and verifiable.

Step 2: Per-label entailment against ground-truth. Let \mathcal{L} be the fixed label set (e.g. 14 CheXpert labels) and let $z_{i,\ell}^* \in \{0, 1\}$ be the ground-truth for label $\ell \in \mathcal{L}$ on study x_i . We then run an LLM-based entailment check that maps the fact set to label-level predictions:

$$\hat{z}_{i,\ell} = \mathbf{1}[\exists s \in \mathcal{F}(\hat{y}_i) \text{ s.t. } \text{entails}(s, \ell) = \text{true}] \quad (14)$$

Table 1. Experimental results on the CheXpert Plus dataset [8] using **RRG task-specific algorithms**. We report per-label **Precision**, **Recall**, and **F1** (14 pathologies). **Train Size** is the number of training samples. Some baselines train on multiple corpora and/or in multiple stages. Best and second best are in **bold** and underline, respectively.

Algorithm	Venue	Precision, Recall, F1	Train Size
R2GenRL [51]	ACL22	0.193, 0.229, 0.196	223K
XProNet [57]	ECCV22	0.314, 0.247, 0.259	223K
MSAT [63]	MICCAI22	0.044, 0.142, 0.057	223K
ORGan [25]	ACL23	0.288, 0.287, 0.277	223K
M2KT [70]	MIA21	0.044, 0.142, 0.058	223K
TIMER [66]	CHIL23	<u>0.345</u> , 0.238, 0.234	223K
CvT2DistilGPT2 [46]	AIM23	0.285, 0.252, 0.246	223K
R2Gen [13]	EMNLP20	0.318, 0.200, 0.181	223K
R2GenCMN [14]	ACL21	0.329, 0.241, 0.231	223K
Zhu et al. [81]	MICCAI23	0.217, 0.308, 0.205	223K
CAMANet [58]	IEEE JBHI23	0.328, 0.224, 0.216	223K
ASGMD [68]	ESWA24	0.146, 0.108, 0.055	223K
Token-Mixer [71]	IEEE TMI23	0.309, 0.270, 0.288	223K
PromptMRG [27]	AAAI24	0.258, 0.265, 0.281	223K
R2GenGPT [65]	Meta-Rad.23	0.315, 0.244, 0.260	223K
WCL [69]	EMNLP21	0.335, 0.259, 0.256	223K
R2GenCSR [60]	arXiv24	0.315, 0.247, 0.259	223K
Wang et al. [61]	VIS INT25	0.175, 0.099, 0.078	223K
CheXagent [15]	arXiv24	0.373, 0.194, 0.186	8.5M
MambaXray-B [62]	CVPR25	0.333, 0.264, 0.273	1.27M
MambaXray-L [62]	CVPR25	0.377 , <u>0.319</u> , <u>0.335</u>	1.27M
VLCI [12]	IEEE TIP25	0.341, 0.175, 0.163	223K
Ours	–	0.237, 0.832 , 0.341	1K

for all $\ell \in \mathcal{L}$. Explicit contradictions to ℓ are treated as false positives for that label (discouraging unsupported claims).

Step 3: A dense, interpretable reward. Based on $(\hat{z}_{i,\ell}, z_{i,\ell}^*)_{\ell \in \mathcal{L}}$, we compute standard per-instance precision P_i and recall R_i , and the reward as an F_β score

$$r(x_i, \hat{y}_i) = F_{\beta,i} = \frac{(1 + \beta^2) P_i R_i}{\beta^2 P_i + R_i + \xi}, \quad (15)$$

with $\beta > 1$ placing more weight on recall (penalizing missed positive findings) and $\beta < 1$ emphasizing precision; ξ is a small constant for stability. The reward is dense and label-wise interpretable, directly supervising diagnostic correctness while remaining token-efficient. It requires no critic, no auxiliary reward model, nor long reasoning traces. By anchoring each sentence to specific clinical facts and aligning them with ground-truth labels, the FactS Reward reduces unsupported claims and improves coverage of required findings, providing a faithful signal for OraPO.

4. Experiments

4.1. Experimental Setup

Datasets. CheXpert Plus [8] is a recent large-scale paired image–text resource that links chest X-ray DICOMs to fully de-identified radiology reports, organized into report subsections and annotated for 14 target pathologies (i.e. disease labels). The public release includes $\sim 223K$ image–report

Table 2. Experimental Results on the CheXpert Plus benchmark [8] across diverse **LLMs/VLMs**, all supervised fine-tuned with R2GenGPT [65] on CheXpert Plus. We report macro **Precision**, **Recall**, and **F1** (14 pathologies). The **Params** listed denotes the parameters that need to be tuned in the training phase. **FT-Size** indicates the number of samples used for fine-tuning. Best and second best are in **bold** and underline, respectively.

LLM/VLM	Year	Precision, Recall, F1	Params	FT-Size
Vicuna-V1.5 [78]	2023	0.334, 0.258, 0.276	6.7B	223K
Qwen-1.5 [3]	2024	0.303, 0.233, 0.241	7.7B	223K
Qwen-2 [3]	2024	0.313, 0.269, 0.261	7.6B	223K
InternLM [7]	2024	0.307, <u>0.274</u> , <u>0.284</u>	7.3B	223K
Llama-2 (7B) [56]	2023	0.315, 0.244, 0.260	6.7B	223K
Llama-2 (13B) [56]	2023	0.321, 0.254, 0.267	13.0B	223K
Llama-3 [18]	2024	0.306, 0.232, 0.222	8.0B	223K
Llama-3.1 [18]	2024	0.295, 0.251, 0.242	8.0B	223K
GPT2-Medium [52]	2019	0.358 , 0.186, 0.165	354M	223K
Orca-2 (7B) [43]	2023	0.330, 0.251, 0.271	6.7B	223K
Orca-2 (13B) [43]	2023	0.317, 0.242, 0.257	13.0B	223K
Deepseek-LLM [5]	2024	<u>0.336</u> , 0.256, 0.253	6.9B	223K
Yi-1.5 (6B) [73]	2024	0.322, 0.229, 0.226	6.1B	223K
Yi-1.5 (9B) [73]	2024	<u>0.336</u> , 0.241, 0.243	8.8B	223K
InternVL-2 [7]	2023	0.196, 0.127, 0.132	8.0B	223K
MiniCPM-V2.5 [72]	2024	0.254, 0.152, 0.122	8.4B	223K
Ours	–	0.237, 0.832 , 0.341	3B	1K

Table 3. Ablation on CheXpert Plus [8]: Impact of the **FactS** reward and **OraPO**. The first row indicates the base Qwen2.5-VL-3B-Instruct [4] direct test results, without any fine-tuning. The second row corresponds to a naïve GRPO-based RLHF baseline using accuracy as the reward [21]. We report per-label **Precision**, **Recall**, and **F1** across 14 findings.

FactS	OraPO	Train Size	Precision, Recall, F1
×	×	0	0.097, 0.104, 0.034
×	×	1,000	0.026, 0.162, 0.089
✓	×	1,000	0.204, 0.605, 0.291
✓	✓	400	0.217, 0.732, 0.296
✓	✓	1,000	0.237 , 0.832 , 0.341

pairs across $\sim 187.7k$ studies and $\sim 64.7k$ patients, totaling $\sim 36M$ report tokens. For data-efficient reinforcement fine-tuning, we subsample a pool of 1,000 studies with a balanced ground-truth label set via CheXpert labeller [26]. We also exclude reports with missing sections. Following recent works [62], we report results on the test split and extract labels from both generated and GT reports by the CheXpert labeller.

Baselines. Following the recent CheXpert Plus benchmark study [62], we compare our proposed approach against a broad suite of methods: **22 task-specific RRG models** spanning diverse architectures: ORGan [25], M2KT [70], ASGMD [68], Token-Mixer [71], PromptMRG [27], R2GenRL [51], XProNet [57], MSAT [63], TIMER [66], CvT2DistilGPT2 [46], R2Gen [13], R2GenCMN [14], Zhu et al. [81], CAMANet [58], R2GenGPT [65], WCL [69], VLCI [12], Wang et al. [61], R2GenCSR [60], and the

recent MambaXray-B/L [62], as well as CheXagent [15], and **16 open-source LLMs/VLMs**, including Vicuna-7B [78], Qwen1.5-7B and Qwen2-7B-Instruct [3], InternLM-7B [7], Llama-2 (7B/13B) [56], Llama-3/3.1 (8B) [18], GPT-2 Medium [52], Orca-2 (7B/13B) [43], DeepSeek-LLM-7B-Chat [5], Yi-1.5 (6B/9B) [73], InternVL-2 [7], and MiniCPM-V2.5 [72]. All task-specific algorithms are fine-tuned on at least the full CheXpert Plus training set, and some of them on multi-source corpora. Thus, our 1K training set represents $\sim 0.45\%$ of the standard 223K split; and only $\sim 0.079\%$ of the 1.27M used by MambaXray [12], which is the current SOTA model.

Evaluation Metric. We follow [62] to report *clinical effectiveness* as macro-averaged over labels: for each of the 14 conditions we compute Precision, Recall, and F1 on the test set, then take the unweighted mean across labels so frequent and rare conditions contribute equally.

Implementation Details. We fine-tune a **3B** Qwen-2.5-VL policy [4] on the **1,000** CheXpert Plus studies in an **RL-only** setting (no SFT/alignment), using Hugging Face TRL’s GRPOTrainer with transformers and accelerate. Training runs on four NVIDIA A10 GPUs (24 GB) with PyTorch 2.7.1/CUDA 12.1. We empirically set batch size $B = 16$. For each prompt, we sample $K = 8$ completions, compute the **FactS** reward per completion, and optimize the objective in Eq. (11): GRPO provides the default learning signal, while DPO is invoked adaptively via the ZRR schedule. To prioritize GRPO yet correct hard, zero-reward cases, we map the EMA zero-reward rate $\tilde{z}_i^{(t)}$ with $\alpha = 0.5$ in Eq. (9) to a bounded mixing weight $w_i^{(t)}$ in Eq. (10) with $w_{\min} = 0.05$, $w_{\max} = 0.15$, $\gamma = 2$. Thus, $w_i^{(t)} \rightarrow w_{\max}$ only when a prompt’s ZRR approaches 1 (no usable GRPO signal), and it quickly decays toward w_{\min} once GRPO yields non-zero rewards, ensuring GRPO dominates ordinary updates and DPO remains a light, targeted aid. We adopt two length-aware variants to handle variable-length reports: DR.GRPO [38] to mitigate length bias in on-policy updates, and LN-DPO [2] to normalize preference margins by sequence length.

4.2. Main Results and Analysis on CheXpert Plus

Against RRG task-specific algorithms. As shown in Tab. 1, **OraPO+FactS** sets the new SOTA **F1 = 0.341 (best)** and **Recall = 0.832 (best)** on CheXpert Plus, significantly surpassing best-performing baselines by **+160.8%** in recall. When compared with the most recent baseline, VLCI, our proposed method outperforms VLCI by **+109.2%** in F1 and **+375.4%** in recall. While our precision trails MambaXray-L, this is a deliberate trade-off between emphasizing per-finding coverage and accurate statements of detected findings. In practice, recall-oriented drafts are preferred, as radiologists perform the final review, they often

prefer high-sensitivity assistance [23]. Overall, our method sets the new SOTA performance in F1 and recall, with **three orders of magnitude** less training data.

Against Alignment-based SFT for LLM/VLM. In this experiment, we compare our framework against R2GenGPT [65], a popular alignment-based SFT approach that is widely used for training large LLM/VLM. In this approach, a visual encoder is aligned with a language model into the same space via supervised fine-tuning on paired image-report data. We report the performance of R2GenGPT [65] with different LLM/VLM backbones in Tab. 2. Our approach is trained with a compact **3B** policy on **1K** CheXpert Plus samples. Under this small-data setup, **OraPO** attains **F1 = 0.341** and **Recall = 0.832**, significantly outperforming larger aligned backbones trained on 223K: F1 improves over InternLM by **+20.1%** and over Qwen-2 (0.261) by **+30.7%**; recall improves over InternLM by **+203.6%** and over GPT-2 Medium by **+347.3%**. These results validate that our proposed **OraPO** with fact-level supervision is a superior learning paradigm than standard vision–language alignment, achieving higher performance with **less than half backbone parameters** and **markedly less training data**.

4.3. Ablation Study

To study the effectiveness and efficiency of our proposed method, we evaluate four model variants on CheXpert Plus using macro **Precision**, **Recall**, and **F1**. As reported in Tab. 3, the second row is a naïve GRPO-based RLHF baseline that uses *accuracy* as reward (as in DeepSeek-R1 [21]), which yields only marginal gains over the base model without any domain-specific training (row 1). Adding **FactS** to GRPO (row 3) lifts F1 from 0.089 to 0.291 (+227%), Recall from 0.162 to 0.605 (+274%), and Precision from 0.026 to 0.204 (+685%), showing that fact-level entailment provides dense, clinically aligned supervision. Layering **OraPO** on top (row 5) further improves F1 to 0.341 (+17.2% vs. **FactS**-only), with Recall improved by (+37.5%) and Precision improved by (+16.2%). Notably, **OraPO+FactS** with only **400** studies (row 4) attains **F1 = 0.296**, **Precision = 0.217** and **Recall = 0.732**—surpassing the **FactS**-only 1K setting (**F1 = 0.291**, **Precision = 0.204**, and **Recall = 0.605**)—providing evidence of OraPO’s superb *data efficiency*. Overall, **FactS** supplies faithful, sentence-level rewards, while **OraPO** converts zero-reward groups into preference updates, yielding higher precision & recall and earlier learning on scarce yet clinically important signals.

5. Conclusion

In this work, we present **OraPO**, an oracle-educated RL training algorithm for high-quality radiology report generation under tight data and compute budgets. To our knowl-

edge, we are the *first to couple DPO with GRPO*: when GRPO exploration fails, we recycle those rollouts as negatives and apply a lightweight DPO step to recover useful gradients. In parallel, we design the **Facts** reward to provide dense, fact-level, clinically faithful supervision tailored to RRG. Comprehensive experiments show **OraPO setting the new SOTA performance while using 2–3 orders of magnitude fewer training samples**.

We have identified a number of promising future work directions. (i) While designed for the RRG task, **OraPO** can be applied to other hard, general-domain tasks where vanilla GRPO struggles with sparse success signals (*e.g.*, multi-step mathematical reasoning and code synthesis). We will extend experiments to other tasks to validate the effectiveness of **OraPO**. (ii) Due to compute constraints, our results currently are limited to a 3B backbone VLM with only 1K studies for training. We plan to study **OraPO**'s scaling behavior across model sizes and data/training budgets. (iii) While our reward design already bridges the gap between verifiable and non-verifiable model outputs by leveraging LLMs as a judge, it still falls short of handling genuinely non-verifiable rewards. Inspired by the recent *Rubrics as Rewards* technique [20], we plan to extend our methodology to address the challenge of non-verifiable reward modeling. (iv) **Facts** mainly scores disease presence/absence and underweights attributes (location, laterality, size/severity, temporal change). We will design a more fine-grained fact-to-attribute entailment reward for addressing the misalignment issue on diagnostic attributes.

References

- [1] Julián Nicolás Acosta, Siddhant Dogra, Subathra Adithan, Kay Wu, Michael Moritz, Stephen Kwak, and Pranav Rajpurkar. The impact of AI assistance on radiology reporting: A pilot study using simulated AI draft reports. *CoRR*, abs/2412.12042, 2024. 2
- [2] Kian Ahrabian, Xihui Lin, Barun Patra, Vishrav Chaudhary, Alon Benhaim, Jay Pujara, and Xia Song. A practical analysis of human alignment with *po. In *Findings of the Association for Computational Linguistics (NAACL)*, pages 8013–8021, 2025. 7
- [3] Jinze Bai, Shuai Bai, Yunfei Chu, Zeyu Cui, Kai Dang, and et al. Qwen technical report. *CoRR*, abs/2309.16609, 2023. 6, 7
- [4] Shuai Bai, Keqin Chen, and et al. Qwen2.5-vl technical report. *CoRR*, abs/2502.13923, 2025. 6, 7
- [5] Xiao Bi, Deli Chen, and et al. Deepseek LLM: scaling open-source language models with longtermism. *CoRR*, abs/2401.02954, 2024. 6, 7
- [6] Shenshen Bu, Taiji Li, Yuedong Yang, and Zhiming Dai. Instance-level expert knowledge and aggregate discriminative attention for radiology report generation. In *Proc. IEEE Conference on Computer Vision and Pattern Recognition (CVPR)*, pages 14194–14204, 2024. 3
- [7] Zheng Cai, Maosong Cao, Haojiong Chen, Kai Chen, Keyu Chen, Xin Chen, and et al. Internlm2 technical report. *CoRR*, abs/2403.17297, 2024. 6, 7
- [8] Pierre J. Chambon, Jean-Benoit Delbrouck, Thomas Sounack, Shih-Cheng Huang, Zhihong Chen, Maya Varma, Steven Q. H. Truong, Chu The Chuong, and Curtis P. Langlotz. Chexpert plus: Augmenting a large chest x-ray dataset with text radiology reports, patient demographics and additional image formats. *CoRR*, abs/2405.19538, 2024. 2, 6
- [9] Aili Chen, Aonian Li, , and et al. Minimax-m1: Scaling test-time compute efficiently with lightning attention. *CoRR*, abs/2506.13585, 2025. 3
- [10] Hardy Chen, Haoqin Tu, Fali Wang, Hui Liu, Xianfeng Tang, Xinya Du, Yuyin Zhou, and Cihang Xie. SFT or rl? an early investigation into training rl-like reasoning large vision-language models. *CoRR*, abs/2504.11468, 2025. 2
- [11] Liang Chen, Xueting Han, Li Shen, Jing Bai, and Kam-Fai Wong. Beyond two-stage training: Cooperative sft and rl for llm reasoning. *CoRR*, abs/2509.06948, 2025. 2
- [12] Weixing Chen, Yang Liu, Ce Wang, Jiarui Zhu, Guanbin Li, Cheng-Lin Liu, and Liang Lin. Cross-modal causal representation learning for radiology report generation. *IEEE Transactions on Image Processing*, 34:2970–2985, 2025. 6, 7
- [13] Zhihong Chen, Yan Song, Tsung-Hui Chang, and Xiang Wan. Generating radiology reports via memory-driven transformer. In *Proc. Conference on Empirical Methods in Natural Language Processing (EMNLP)*, pages 1439–1449, 2020. 3, 6
- [14] Zhihong Chen, Yaling Shen, Yan Song, and Xiang Wan. Cross-modal memory networks for radiology report generation. In *Proc. Annual Meeting of the Association for Computational Linguistics and International Joint Conference on Natural Language Processing, (ACL/IJCNLP)*, pages 5904–5914, 2021. 6
- [15] Zhihong Chen, Maya Varma, Jean-Benoit Delbrouck, Magdalin Paschali, Louis Blankemeier, Dave Van Veen, Jeya Maria Jose Valanarasu, Alaa Youssef, Joseph Paul Cohen, Eduardo Pontes Reis, Emily Bao Tsai, Andrew Johnston, Cameron Olsen, Tanishq Mathew Abraham, Sergios Gatidis, Akshay S. Chaudhari, and Curtis P. Langlotz. Chexagent: Towards a foundation model for chest x-ray interpretation. *CoRR*, abs/2401.12208, 2024. 6, 7
- [16] DeepSeek-AI, Daya Guo, Dejian Yang, Haowei Zhang, Junxiao Song, Ruoyu Zhang, and et al. Deepseek-rl: Incentivizing reasoning capability in llms via reinforcement learning. *CoRR*, abs/2501.12948, 2025. 2
- [17] Dina Demner-Fushman, Marc D. Kohli, Marc B. Rosenman, Sonya E. Shooshan, Laritza Rodriguez, Sameer K. Antani, George R. Thoma, and Clement J. McDonald. Preparing a collection of radiology examinations for distribution and retrieval. *Journal of the American Medical Informatics Association*, 23(2):304–310, 2016. 2
- [18] Abhimanyu Dubey, Abhinav Jauhri, Abhinav Pandey, Abhishek Kadian, Ahmad Al-Dahle, and et al. The llama 3 herd of models. *CoRR*, abs/2407.21783, 2024. 6, 7
- [19] Yash Goyal, Tejas Khot, Aishwarya Agrawal, Douglas Summers-Stay, Dhruv Batra, and Devi Parikh. Making the

- V in VQA matter: Elevating the role of image understanding in visual question answering. *International Journal of Computer Vision*, 127(4):398–414, 2019. 4
- [20] Anisha Gunjal, Anthony Wang, Elaine Lau, Vaskar Nath, Bing Liu, and Sean Hendryx. Rubrics as rewards: Reinforcement learning beyond verifiable domains, 2025. 8
- [21] Daya Guo, Dejian Yang, Haowei Zhang, Junxiao Song, Peiyi Wang, Qihao Zhu, Runxin Xu, Ruoyu Zhang, Shirong Ma, Xiao Bi, et al. Deepseek-r1 incentivizes reasoning in llms through reinforcement learning. *Nature*, 645(8081):633–638, 2025. 3, 4, 6, 7
- [22] Ibrahim Ethem Hamamci, Sezgin Er, and Bjoern H. Menze. Ct2rep: Automated radiology report generation for 3d medical imaging. In *Proc. Medical Image Computing and Computer Assisted Intervention (MICCAI)*, pages 476–486, 2024. 3
- [23] Nathaniel Hendrix, Kathryn P Lowry, Joann G Elmore, William Lotter, Gregory Sorensen, William Hsu, Geraldine J Liao, Sana Parsian, Suzanne Kolb, Arash Naeim, et al. Radiologist preferences for artificial intelligence-based decision support during screening mammography interpretation. *Journal of the American College of Radiology*, 19(10):1098–1110, 2022. 7
- [24] Jiwoo Hong, Noah Lee, and James Thorne. ORPO: monolithic preference optimization without reference model. In *Proc. Conference on Empirical Methods in Natural Language Processing (EMNLP)*, pages 11170–11189, 2024. 3
- [25] Wenjun Hou, Kaishuai Xu, Yi Cheng, Wenjie Li, and Jiang Liu. ORGAN: observation-guided radiology report generation via tree reasoning. In *Proc. Annual Meeting of the Association for Computational Linguistics (ACL)*, pages 8108–8122, 2023. 6
- [26] Jeremy Irvin, Pranav Rajpurkar, and et al. Chexpert: A large chest radiograph dataset with uncertainty labels and expert comparison. In *Proc. Conference on Artificial Intelligence (AAAI)*, pages 590–597, 2019. 6
- [27] Haibo Jin, Haoxuan Che, Yi Lin, and Hao Chen. Promptmrg: Diagnosis-driven prompts for medical report generation. In *Proc. Conference on Artificial Intelligence*, pages 2607–2615, 2024. 6
- [28] Baoyu Jing, Pengtao Xie, and Eric P. Xing. On the automatic generation of medical imaging reports. In *Proc. Annual Meeting of the Association for Computational Linguistics (ACL)*, pages 2577–2586, 2018. 3
- [29] Alistair E. W. Johnson, Tom J. Pollard, Seth J. Berkowitz, Nathaniel R. Greenbaum, Matthew P. Lungren, Chih-ying Deng, Roger G. Mark, and Steven Horng. MIMIC-CXR: A large publicly available database of labeled chest radiographs. *CoRR*, abs/1901.07042, 2019. 2, 3
- [30] Yunsoo Kim, Jinge Wu, Yusuf Abdulle, Yue Gao, and Honghan Wu. Enhancing human-computer interaction in chest x-ray analysis using vision and language model with eye gaze patterns. In *Proc. Medical Image Computing and Computer Assisted Intervention (MICCAI)*, pages 184–194. Springer, 2024. 2
- [31] Alan Lee and Harry Tong. Reinforcement learning for LLM reasoning under memory constraints. *CoRR*, abs/2504.20834, 2025. 2, 3
- [32] Chunyuan Li, Cliff Wong, Sheng Zhang, Naoto Usuyama, Haotian Liu, Jianwei Yang, Tristan Naumann, Hoifung Poon, and Jianfeng Gao. Llava-med: Training a large language-and-vision assistant for biomedicine in one day. In *Proc. Advances in Neural Information Processing Systems (NeurIPS)*, 2023. 2, 3
- [33] Yuan Li, Xiaodan Liang, Zhiting Hu, and Eric P. Xing. Hybrid retrieval-generation reinforced agent for medical image report generation. In *Proc. Advances in Neural Information Processing Systems (NeurIPS)*, pages 1537–1547, 2018. 2
- [34] Tsung-Yi Lin, Michael Maire, Serge J. Belongie, James Hays, Pietro Perona, Deva Ramanan, Piotr Dollár, and C. Lawrence Zitnick. Microsoft COCO: common objects in context. In *Proc. European Conference on Computer Vision (ECCV)*, pages 740–755, 2014. 4
- [35] Chang Liu, Yuanhe Tian, Weidong Chen, Yan Song, and Yongdong Zhang. Bootstrapping large language models for radiology report generation. In *Proc. Conference on Artificial Intelligence (AAAI)*, pages 18635–18643, 2024. 3
- [36] Kang Liu, Zhuoqi Ma, Xiaolu Kang, Yunan Li, Kun Xie, Zhicheng Jiao, and Qiguang Miao. Enhanced contrastive learning with multi-view longitudinal data for chest x-ray report generation. In *Proc. IEEE Conference on Computer Vision and Pattern Recognition (CVPR)*, pages 10348–10359, 2025. 3
- [37] Mingyang Liu, Gabriele Farina, and Asuman E. Ozdaglar. UFT: unifying supervised and reinforcement fine-tuning. *CoRR*, abs/2505.16984, 2025. 2
- [38] Zichen Liu, Changyu Chen, Wenjun Li, Penghui Qi, Tianyu Pang, Chao Du, Wee Sun Lee, and Min Lin. Understanding r1-zero-like training: A critical perspective. *CoRR*, abs/2503.20783, 2025. 3, 7
- [39] Xingtai Lv, Yuxin Zuo, and et al. Towards a unified view of large language model post-training. *CoRR*, abs/2509.04419, 2025. 2
- [40] Lu Ma, Hao Liang, Meiyi Qiang, Lexiang Tang, Xiaochen Ma, Zhen Hao Wong, Junbo Niu, Chengyu Shen, Runming He, Bin Cui, and Wentao Zhang. Learning what reinforcement learning can’t: Interleaved online fine-tuning for hardest questions. *CoRR*, abs/2506.07527, 2025. 2
- [41] Yu Meng, Mengzhou Xia, and Danqi Chen. Simpo: Simple preference optimization with a reference-free reward. In *Proc. Advances in Neural Information Processing Systems (NeurIPS)*, 2024. 3
- [42] Sewon Min, Kalpesh Krishna, Xinxu Lyu, Mike Lewis, Wentao Yih, Pang Wei Koh, Mohit Iyyer, Luke Zettlemoyer, and Hannaneh Hajishirzi. Factscore: Fine-grained atomic evaluation of factual precision in long form text generation. In *Proc. Conference on Empirical Methods in Natural Language Processing (EMNLP)*, pages 12076–12100, 2023. 2, 5
- [43] Arindam Mitra, Luciano Del Corro, and et al. Orca 2: Teaching small language models how to reason. *CoRR*, abs/2311.11045, 2023. 6, 7
- [44] Yasuhide Miura, Yuhao Zhang, Emily Bao Tsai, Curtis P. Langlotz, and Dan Jurafsky. Improving factual completeness and consistency of image-to-text radiology report generation. In *Proc. Conference of the North American Chapter*

- of the Association for Computational Linguistics: Human Language Technologies, (NAACL-HLT), pages 5288–5304, 2021. 2
- [45] Youssef Mroueh, Nicolas Dupuis, Brian Belgodere, Apoorva Nitsure, Mattia Rigotti, Kristjan H. Greenewald, Jiri Navrátil, Jerret Ross, and Jesus Rios. Revisiting group relative policy optimization: Insights into on-policy and off-policy training. *CoRR*, abs/2505.22257, 2025. 2, 3
- [46] Aaron Nicolson, Jason Dowling, and Bevan Koopman. Improving chest x-ray report generation by leveraging warm starting. *Artificial Intelligence*, 144:102633, 2023. 6
- [47] Aaron Nicolson, Jinghui Liu, Jason Dowling, Anthony N. Nguyen, and Bevan Koopman. e-health CSIRO at RRG24: entropy-augmented self-critical sequence training for radiology report generation. In *Proc. Workshop on Biomedical Natural Language Processing (BioNLP@ACL)*, pages 99–104, 2024. 2
- [48] John Nightingale, Stephen Eddy, Beverley Snaith, Tracy Stevens, Richard Appleyard, and Stephen Kelly. Establishing the size and configuration of the imaging support workforce: a census of national workforce data in england. *BJR—Open*, 6(1):tzae026, 2024. 2
- [49] OpenAI. GPT-4 technical report. *CoRR*, abs/2303.08774, 2023. 5
- [50] Sang-Jun Park, Keun-Soo Heo, Dong-Hee Shin, Young-Han Son, Ji-Hye Oh, and Tae-Eui Kam. DART: disease-aware image-text alignment and self-correcting re-alignment for trustworthy radiology report generation. In *Proc. IEEE Conference on Computer Vision and Pattern Recognition (CVPR)*, pages 15580–15589, 2025. 3
- [51] Han Qin and Yan Song. Reinforced cross-modal alignment for radiology report generation. In *Findings of the Association for Computational Linguistics (ACL Findings)*, pages 448–458, 2022. 6
- [52] Alec Radford, Jeff Wu, Rewon Child, David Luan, Dario Amodei, and Ilya Sutskever. Language models are unsupervised multitask learners. Technical report, OpenAI, San Francisco, CA, 2019. Technical report. 6, 7
- [53] James V. Rawson, Dana Smetherman, and Eric Rubin. Short-term strategies for augmenting the national radiologist workforce. *American Journal of Roentgenology*, 222(6):e2430920, 2024. 2
- [54] Zhihong Shao, Peiyi Wang, Qihao Zhu, Runxin Xu, Junxiao Song, Mingchuan Zhang, Y. K. Li, Y. Wu, and Daya Guo. Deepseekmath: Pushing the limits of mathematical reasoning in open language models. *CoRR*, abs/2402.03300, 2024. 2, 3, 4
- [55] Vaishnavi Shrivastava, Ahmed Awadallah, Vidhisha Balachandran, Shivam Garg, Harkirat Behl, and Dimitris Papailiopoulos. Sample more to think less: Group filtered policy optimization for concise reasoning. *CoRR*, abs/2508.09726, 2025. 2, 3
- [56] Hugo Touvron, Louis Martin, Kevin Stone, Peter Albert, Amjad Almahairi, and et al. Llama 2: Open foundation and fine-tuned chat models. *CoRR*, abs/2307.09288, 2023. 6, 7
- [57] Jun Wang, Abhir Bhalerao, and Yulan He. Cross-modal prototype driven network for radiology report generation. In *Proc. European Conference on Computer Vision (ECCV)*, pages 563–579, 2022. 6
- [58] Jun Wang, Abhir Bhalerao, Terry Yin, Simon See, and Yulan He. Camanet: Class activation map guided attention network for radiology report generation. *IEEE Journal of Biomedical and Health Informatics*, 28(4):2199–2210, 2024. 6
- [59] Liangyu Wang, Huanyi Xie, Xinhai Wang, Tianjin Huang, Mengdi Li, and Di Wang. Infinite sampling: Efficient and stable grouped RL training for large language models. *CoRR*, abs/2506.22950, 2025. 3
- [60] Xiao Wang, Yuehang Li, Fuling Wang, Shiao Wang, Chuanfu Li, and Bo Jiang. R2gensr: Retrieving context samples for large language model based x-ray medical report generation. *CoRR*, abs/2408.09743, 2024. 6
- [61] Xiao Wang, Yuehang Li, Wentao Wu, Jiandong Jin, Yao Rong, Bo Jiang, Chuanfu Li, and Jin Tang. Pre-training on high-resolution x-ray images: an experimental study. *Visual Intelligence*, 3(1), 2025. 6
- [62] Xiao Wang, Fuling Wang, Yuehang Li, Qingchuan Ma, Shiao Wang, Bo Jiang, and Jin Tang. Cxpmrg-bench: Pre-training and benchmarking for x-ray medical report generation on chexpert plus dataset. In *Proc. IEEE Conference on Computer Vision and Pattern Recognition (CVPR)*, pages 5123–5133, 2025. 2, 3, 6, 7
- [63] Zhanyu Wang, Mingkan Tang, Lei Wang, Xiu Li, and Luping Zhou. A medical semantic-assisted transformer for radiographic report generation. In *Proc. Medical Image Computing and Computer Assisted Intervention (MICCAI)*, pages 655–664, 2022. 6
- [64] Zhanyu Wang, Lingqiao Liu, Lei Wang, and Luping Zhou. Metransformer: Radiology report generation by transformer with multiple learnable expert tokens. In *Proc. IEEE Conference on Computer Vision and Pattern Recognition*, pages 11558–11567, 2023. 2
- [65] Zhanyu Wang, Lingqiao Liu, Lei Wang, and Luping Zhou. R2gengpt: Radiology report generation with frozen llms. *Meta-Radiology*, 1(3):100033, 2023. 6, 7
- [66] Yuexin Wu, I-Chan Huang, and Xiaolei Huang. Token imbalance adaptation for radiology report generation. In *Proc. Conference on Health, Inference, and Learning (CHIL)*, pages 72–85, 2023. 6
- [67] Teng Xiao, Yige Yuan, Huaisheng Zhu, Mingxiao Li, and Vasant G. Honavar. Cal-dpo: Calibrated direct preference optimization for language model alignment. In *Proc. Advances in Neural Information Processing Systems (NeurIPS)*, 2024. 3
- [68] Youyuan Xue, Yun Tan, Ling Tan, Jiaohua Qin, and Xuyi Xiang. Generating radiology reports via auxiliary signal guidance and a memory-driven network. *Expert Systems With Applications*, 237(Part B):121260, 2024. 6
- [69] An Yan, Zexue He, Xing Lu, Jiang Du, Eric Y. Chang, Amilcare Gentili, Julian J. McAuley, and Chun-Nan Hsu. Weakly supervised contrastive learning for chest x-ray report generation. In *Proc. Conference on Empirical Methods in Natural Language Processing (EMNLP)*, pages 4009–4015, 2021. 6
- [70] Shuxin Yang, Xian Wu, Shen Ge, Zhuozhao Zheng, S. Kevin Zhou, and Li Xiao. Radiology report generation with a

- learned knowledge base and multi-modal alignment. *Medical Image Analysis*, 86:102798, 2023. 6
- [71] Yan Yang, Jun Yu, Zhenqi Fu, Ke Zhang, Ting Yu, Xianyun Wang, Hanliang Jiang, Junhui Lv, Qingming Huang, and Weidong Han. Token-mixer: Bind image and text in one embedding space for medical image reporting. *IEEE Transactions on Medical Imaging*, 43(11):4017–4028, 2024. 6
- [72] Yuan Yao, Tianyu Yu, and et al. Minicpm-v: A GPT-4V level MLLM on your phone. *CoRR*, abs/2408.01800, 2024. 6, 7
- [73] Alex Young, Bei Chen, and et al. Yi: Open foundation models by 01.ai. *CoRR*, abs/2403.04652, 2024. 6, 7
- [74] Feiyang Yu, Mark Endo, Rayan Krishnan, Ian Pan, Andy Tsai, Eduardo Pontes Reis, Eduardo Kaiser Ururahy Nunes Fonseca, Henrique Min Ho Lee, Zahra Shakeri Hossein Abad, Andrew Y. Ng, Curtis P. Langlotz, Vasantha Kumar Venugopal, and Pranav Rajpurkar. Evaluating progress in automatic chest x-ray radiology report generation. *Patterns*, 4(9):100802, 2023. 2
- [75] Qiyang Yu, Zheng Zhang, Ruofei Zhu, Yufeng Yuan, Xiaochen Zuo, Yu Yue, Tiantian Fan, Gaohong Liu, Lingjun Liu, Xin Liu, Haibin Lin, Zhiqi Lin, Bole Ma, Guangming Sheng, Yuxuan Tong, Chi Zhang, Mofan Zhang, Wang Zhang, Hang Zhu, Jinhua Zhu, Jiase Chen, Jiangjie Chen, Chengyi Wang, Hongli Yu, Weinan Dai, Yuxuan Song, Xi-angpeng Wei, Hao Zhou, Jingjing Liu, Wei-Ying Ma, Ya-Qin Zhang, Lin Yan, Mu Qiao, Yonghui Wu, and Mingxuan Wang. DAPO: an open-source LLM reinforcement learning system at scale. *CoRR*, abs/2503.14476, 2025. 2, 3
- [76] Wenhao Zhang, Yuexiang Xie, Yuchang Sun, Yanxi Chen, Guoyin Wang, Yaliang Li, Bolin Ding, and Jingren Zhou. On-policy RL meets off-policy experts: Harmonizing supervised fine-tuning and reinforcement learning via dynamic weighting. *CoRR*, abs/2508.11408, 2025. 2
- [77] Chujie Zheng, Shixuan Liu, , and et al. Group sequence policy optimization. *CoRR*, abs/2507.18071, 2025. 3
- [78] Lianmin Zheng, Wei-Lin Chiang, Ying Sheng, Siyuan Zhuang, Zhanghao Wu, Yonghao Zhuang, Zi Lin, Zhuohan Li, Dacheng Li, Eric P. Xing, Hao Zhang, Joseph E. Gonzalez, and Ion Stoica. Judging llm-as-a-judge with mt-bench and chatbot arena. In *Proc. Advances in Neural Information Processing Systems (NeurIPS)*, 2023. 6, 7
- [79] Han Zhong, Guhao Feng, Wei Xiong, Xinle Cheng, Li Zhao, Di He, Jiang Bian, and Liwei Wang. DPO meets PPO: Reinforced token optimization for RLHF. In *International Conference on Machine Learning Workshop on Models of Human Feedback for AI Alignment (ICML Workshop)*, 2024. 3, 4
- [80] Zijian Zhou, Miaojing Shi, Meng Wei, Oluwatosin Alabi, Zijie Yue, and Tom Vercauteren. Large model driven radiology report generation with clinical quality reinforcement learning. *CoRR*, abs/2403.06728, 2024. 2
- [81] Qingqing Zhu, Tejas Sudharshan Mathai, Pritam Mukherjee, Yifan Peng, Ronald M. Summers, and Zhiyong Lu. Utilizing longitudinal chest x-rays and reports to pre-fill radiology reports. In *Proc. Medical Image Computing and Computer Assisted Intervention (MICCAI)*, pages 189–198, 2023. 6